Vol.7 No.3 July 2024

Journal of Networking and Communication Systems

Received 9 August, Revised 13 August, Accepted 3 September

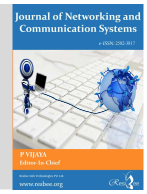

Gradient Boosting Machines for Weather Forecasting: A Huber-Quantile Perspective

Anbhazhagan P

Department of Computer Science and Information Technology
Kebri Dehar University, Ethiopia
Anbhazhagn@kdu.edu.et

Abstract: Weather forecasting is crucial due to its substantial effect on human life. It is frequently done by physical techniques that are unstable to perturbation. Moreover, several traditional models are used for exploring the progressive patterns of meteorological variables. The existing Numerical Weather Prediction (NWP) models acquired unsatisfactory performance because of the unsuitable initial state settings. In addition to this, Machine learning (ML) approaches are considered more robust to perturbations, and hence a new model based on a Gradient Boosting Machine with Huber Quantile Loss (GBM+HQLoss) based on ML is developed for weather forecasting. Firstly, time series data is taken as input and passed to the technical indicator extraction phase. After mining the indicators from input data, a feature selection process is carried out using Information Gain (IG). At last, the weather forecasting is executed by employing a Gradient Boosting Machine (GBM), trained based on Huber Quantile Loss (HQ Loss). Here, the HQ loss is obtained by combining Huber loss and quantum loss. Furthermore, the GBM+HQLoss technique measured a minimum Root Mean Square Error (RMSE) of 0.256, Mean Square Error (MSE) of 0.066, and Mean Absolute Percentage Error (MAPE) of 0.248

Keywords: Weather forecasting, Gradient Boosting Machine, Information Gain, Quantile loss function, Huber loss function.

Nomenclature

Abbreviation	Expansion
NWP	Numerical Weather Prediction
ML	Machine Learning
AI	Artificial Intelligence
ANNs	Artificial Neural Networks
HiSTGNN	Hierarchical Spatio-temporal Graph Neural Network
SFA-LSTM	Spatial Feature Attention Long Short-Term Memory
LSTM	Long Short-Term Memory
TCN	Temporal Convolutional Networks
DL	Deep Learning
WMA	Weighted Moving Average
RSI	Relative Strength Index
MACD	Moving Average Convergence Divergence
ATR	Average True Range
EMA	Exponential Moving Average
SMA	Simple Moving Average
LB	Lower Band
UB	Upper Band

1. Introduction

Weather forecasting is vital to several aspects of human livelihood, and it assists in performing well-informed decision-making in public safety, energy, transportation, and agriculture. The process of predicting the conditions of weather for a specific time and location using the concepts of physics, science, and technology is known as weather forecasting [4]. Weather forecasting is more beneficial in predicting the weather conditions and their effect on our daily life. Moreover, predicting heat waves, rain snow, and floods is regarded as an effective way for the government and the public to prevent dreadful consequences. The information related to these weather conditions is beneficial for maintaining social, environmental, economic, and commercial interests [4]. Furthermore, forecasting is important for handling emergencies,

https://doi.org/10.46253/jnacs.v7i3.a5

averting financial losses, decreasing the effect of extreme weather, and producing constant economic income [2]. Recently, weather forecasting has been established as a cultured science, that depends on various computational approaches and data sources for offering reliable and accurate prediction [3]. Besides, quantitative data that describes the atmosphere's state at a given time is provided by meteorological features, namely temperature, atmospheric pressure, precipitation, wind speed, and humidity that are gathered over a period. These collected data are employed for forecasting the future atmospheric state to understand the process of atmospheric science [4]. More recently, large quantities of daily, hourly, weekly, annual, and monthly weather-related data have been offered by increasing the number of climate monitoring systems, and the data remains transparent [4].

NWP has been developed by applying physical rules to weather predictions. To forecast impending atmospheric movement states, NWP techniques resolve thermodynamics equations and fluid dynamics numerically using supercomputers by utilizing detected meteorological data as initial conditions [2]. Nevertheless, traditional NWP methods could not fully utilize a large quantity of historical observation data to enhance the process of making decisions in sustainable environmental management. Moreover, the main intent of weather forecasting is to plan and execute an ML pipeline for incorporating the essential components for precise, efficient, and data-driven weather forecasting. Effective forecasting is very significant since it is essential for identifying the relations among meteorological features that indirectly contribute to climate change [4]. In addition to this, various ML techniques, like AI models are widely considered as the effective approach for predicting the weather [1]. Furthermore, ANNs are very valuable because of their adaptable learning capability and nature. In addition to this, these ANN approaches are very attractive in application domains where extremely nonlinear phenomena are required to be solved because of the above feature [5]. Moreover, these methods can predict various weather types, such as temperature, wind direction, speed, amount of rainfall, and so on. Further, an ensemble-based approach is an ML algorithm that is exploited by incorporating many ML models, like decision trees, random forests, KNNs, and gradient boost algorithms. Using these ensemble-based models the prediction accuracy can be improved for yielding superior outcomes [15].

This paper aims to present a GBM+HQLoss technique for weather forecasting. Initially, the input time series data is passed to the extraction phase, where the various technical indicators are mined from the data. Following this, the feature is selected based on IG, and lastly, weather forecasting is executed by employing GBM+HQLoss. Here, the training process of GBM is guided based on HQ loss, which is formulated by the integration of Huber loss and Quantile loss.

The contribution of this research is given beneath,

- ***Proposed GBM+HQLoss for weather forecasting:*** To predict the weather, an ML technique based on GBM+HQLoss is formulated. Furthermore, the tuning of GBM is guided based on HQ loss, where HQ Loss is attained by the amalgamation of Quantile Loss and Huber Loss.

The remaining section in this paper is structured as follows: The motivation and the challenges encountered by traditional models are portrayed in Section 2. The description of GBM+HQLoss utilized for weather forecasting is explained in Section 3. The outcomes of GBM+HQLoss are illustrated in Section 4. The conclusion of this research is shown in Section 5.

2. Motivation

Weather forecasting is used to predict the atmospheric conditions at a particular time and location by considering time series data. Precise weather forecasts are essential in many sectors, such as public safety, transportation, disaster management, and agriculture. Various conventional models are presented but fail to forecast the local weather conditions precisely, leading to forecasting errors due to sudden weather changes. Thus, a new ML technique termed GBM+HQLoss has been devised for forecasting the weather. Further, the pros and cons of existing models are described below.

2.1 Literature Review

Niu, D., *et al.* [1] devised a Catboost+ Spatiotemporal Feature + Feature Selection+ Wavelet Packet Denoising (Catboost+ST+FS+WPD) for weather forecasting. This technique achieved high prediction accuracy with less convergence time. However, this approach failed to employ ensemble models and failed to train the hyper-parameters to improve the performance. A Weather model with Masked Autoencoder (W-MAE) was introduced by Man, X., *et al.* for multi-variable weather forecasting. This method was more feasible and implemented various pre-trained models for forecasting, and it provided insights to model long-term dependency. Still, this model did utilize a huge quantity of data for effective training and testing. Ma, M., *et al.* [3] formulated a HiSTGNN for weather forecasting. This approach achieved better performance outcomes on three different real-world meteorological databases. Nevertheless, this method failed to find the optimum solution in multi-meteorological variables optimization and was tested with a relatively small amount of data. SFA-LSTM was presented by Suleman, M.A.R. and Shridevi, S., [4] for weather forecasting. This approach obtained a high prediction accuracy rate and it provided more accurate spatial feature interpretability. However, this technique was complex and required more computational resources for training. Hewage, P., *et al.* [5] developed an LSTM and TCN for weather forecasting. This approach produced satisfactory results and was more applicable for obtaining effective and accurate weather forecasting results. However, this method did not develop a lightweight or short-term weather forecasting system for improving the prediction performance.

2.2 Challenges

The challenges encountered by several traditional models for weather forecasting are described below.

- In [1], the Catboost+ST+FS+WPD approach effectively minimized the computational cost. Nevertheless, this technique failed to incorporate DL methods in the prediction process to improve the prediction performance.
- In [2], the W-MAE technique provided stable forecasting outcomes and outperformed the baseline approach in long forecast time steps. However, this model failed to utilize pre-training techniques for climate forecasting tasks and a wide range of weather.
- In [3], due to the increase in the hierarchical graph's scale, the computational efficiency of HiSTGNN was decreased. Moreover, the HiSTGNN model did not address the large-scale weather station data and failed to examine multi-variable optimization to reduce the complexity.
- Several traditional NWP approaches were formulated for predicting the weather but these models failed to obtain satisfactory performance because of the unsuitable initial state setting. Due to this challenge, the error rate was improved while predicting the weather.

3. Proposed Gradient Boosting Machine with Huber Quantile Loss (GBM+HQLoss) for weather forecasting

Weather is considered a data-intensive, dynamic, continuous, chaotic process making weather forecasting more challenging. Predicting the weather is a more significant and vital process in human life. To predict the weather, a GBM+HQLoss technique has been devised in this work. For that, firstly time series data is fed as input to the technical indicator extraction phase, and here various technical indicators, like WMA [6], RSI [7], MACD [8], Bollinger bands [9], and ATR [10] are mined. After extracting the technical indicators from the data, feature selection is carried out by employing IG [11]. At last, weather forecasting is performed by utilizing the proposed GBM [12][14]. Here, the training of GBM is done based on HQ Loss [13], which is attained by the combination of Huber loss and Quantile loss. The general outline of GBM+HQLoss for weather forecasting is shown in Fig. 1.

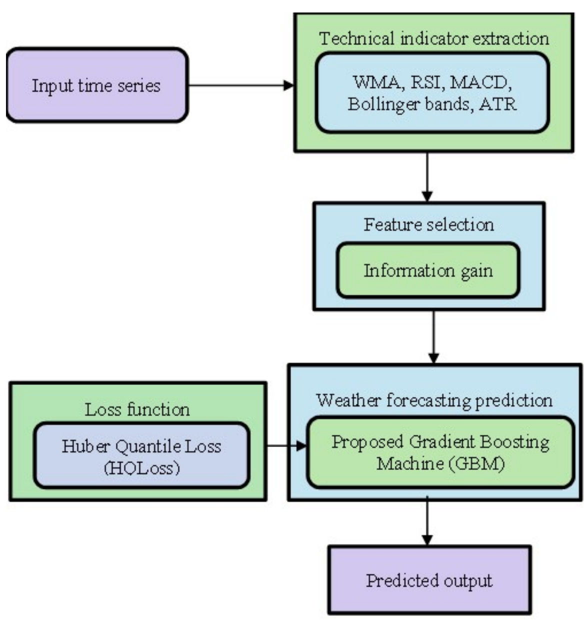

Fig. 1. *General outline of proposed GBM+HQLoss for weather forecasting*

3.1 Data Acquisition

The input time series data is collected from a specified database V, which is formulated by the equation signified below.

$$V = \{V_1, V_2, ..., V_\sigma, ...V_\vartheta\} \tag{1}$$

wherein, the whole number of data contained in the database is epitomized as ϑ and V_σ represents the σ^{th} time series data.

3.2 Technical Indicator Extraction

The technical indicator extraction process is used to enhance operational effectiveness. It is also employed for optimizing the operations and lessening the risks that are related to weather variability. Various technical indicators, like WMA [6], RSI [7], MACD [8], Bollinger bands [9], and ATR [10] are considered and then mined. Moreover, V_σ is taken as input for mining the technical indicators.

(i) WMA

WMA [6] is employed for aggregating several weather parameters over time. WMA mostly relies on artificially created time series, where the value for a specific time is changed by the weighted mean of that value and the values from various former periods. Further, WMA is expressed as,

$$\gamma_1 = \frac{\sum_{q=1}^{u} \left[E(q) * R(q) \right]}{\sum_{q=1}^{u} R(q)} \tag{2}$$

Here, γ_1 symbolizes the WMA, the weather parameter at the time q is denoted as $E(q)$, the number of periods in the moving average is implied as u, and the weight assigned to the parameter at the time q is epitomized as $R(q)$.

(ii) RSI

RSI [7] refers to the frequency of weather changes when correlated to historical averages during a specific period. This indicator is employed for interpreting and analyzing the weather data effectively. Furthermore, the equation of RSI is written as,

$$\gamma_2 = 100 - \frac{100}{1 + RS} \tag{3}$$

where;

$$RS = \frac{T}{Z} \tag{4}$$

Here, T embodies the average temperature increasing over a specified period, Z typifies the average temperature decreases over the same period, and γ_2 signifies RSI.

(iii) MACD

To detect the changes in atmospheric pressure, MACD [8] is utilized. Moreover, MACD is used for providing insights into various changes in climatic conditions and helps to plan and make decisions based on weather conditions. Here, MACD is designated as,

$$\gamma_3 = \sum_{w=1}^{b} EMA_\eta - \sum_{w=1}^{b} EMA_\ell \tag{5}$$

where, γ_3 characterizes the MACD indicator, the number of periods for EMA is denoted as b, $\eta = 12$ and $\ell = 26$ in hours/day. Moreover, the EMA at the time t is formulated as,

$$EMA_t = \delta \cdot M_t + (1 - \delta) \cdot EMA_{t-1} \tag{6}$$

Here, EMA specifies the Exponential Moving Average, δ exemplifies the smoothing factor, and expressed as $\frac{2}{b+1}$, the current humidity level at the time t is characterized as M_t.

(iv) Bollinger bands

Bollinger bands [9] are employed for identifying temperature fluctuations and are exploited for evaluating the instability of the weather produced at a specific time. This indicator is acquired based on historical data, which are utilized for calculating the standard deviation and mean. Here, SMA is employed, where the extreme band's LB and UB are modeled as,

$$UB = SMA(l) + \beta \cdot \sigma(l) \tag{7}$$

$$LB = SMA(l) - \beta \cdot \sigma(l) \tag{8}$$

Here, the value of β is typically set to 2, $\sigma(l)$ indicates the standard deviation of temperature over the time period l, and Bollinger bands are represented as γ_4.

(v) ATR

ATR [10] is used for providing beneficial insights into the instability or stability of weather patterns, which aims to make decisions based on several sectors affected by weather. Further, the expression of ATR is signified as,

$$\gamma_5 = \frac{\sum_{f=1}^{S}(J_{h-f} - Q_{h-f})}{S} \tag{9}$$

wherein, J_{h-f} designates the highest temperature over the period, the forecasted temperature is implied as h, the overall number of time period is signified as S, Q_{h-f} typifies the lowest temperature over the period, and γ_5 symbolizes the mined ATR.

In addition to this, the afore-mentioned features are combined for acquiring a feature vector γ, which is articulated as,

$$\gamma = \{\gamma_1, \gamma_2, \gamma_3, \gamma_4, \gamma_5\} \tag{10}$$

3.3 Feature Selection

Feature selection is used to select and recognize the most applicable features for predicting the accurate conditions of weather. Furthermore, the performance of the model can be enhanced by reducing the overfitting issue. Here, the feature vector γ is taken as input, and IG is utilized for selecting the feature. To examine the reduction in entropy about the predicted variable, IG [11] is employed. Moreover, the IG is calculated based on the difference between the original entropy and weighted entropy from every branch, which is formulated as,

$$G(a, p) = \xi(a) - \xi(a \mid p) \tag{11}$$

wherein, IG is typified as G, a implies the class label, p embodies feature, $\xi(a \mid p)$ indicates the probability of class a for a particular feature p, $\hbar_g$ characterizes features selected based on IG, and the entropy of the class label is represented as $\xi(a)$.

3.4 Weather Forecasting Using GBM+Hq loss

GBM [12] [14] is made in parallel by employing randomized decision trees, and it is considered a simple framework. GBM is a progressive ensemble learning approach, which is employed for classification and regression tasks. This network mostly obtains better performance and has better capability in learning complex patterns. Moreover, GBM is also utilized for decreasing the overfitting issues, which makes the database more suitable. Consider, W training samples $H = \{(d_1, z_1), \ldots, (d_v, z_v)\}$, and here a feature vector with s features is represented by d_κ and it belongs to the set $A \subset \mathrm{R}_e^s$. Additionally, the observed outcomes are represented as $z_\kappa \in \mathrm{R}_e$, and is signified as $z_\kappa = \varsigma(d_\kappa) + \mu$, where random noise with unknown finite variance and expectation 0 is designated as μ and ς denotes residual. Here, the ML is employed for contrasting a regression method or an approximation D of j^{th} function, which reduces the expected loss function. Further, the HQ loss function is utilized for the tuning process of the GBM network, which is generated by the incorporation of the Quantile loss function [13] and the Huber loss function [13] as given below

$$B = \varpi_1(B_C) + \varpi_2(B_N) \tag{12}$$

Here, the HQ loss function is implied as B, the scaling factors are symbolized as ϖ_1 and ϖ_2, B_C represents the Huber loss, B_N epitomizes the quantile loss.

Moreover, the expressions of Huber loss and quantile loss are given in equation (13) and (14).

$$B_C = \begin{cases} \frac{1}{2}(v - r)^2 & ; \ |v - r| \le \omega \\ \omega\left(|v - r| - \omega/2\right) & ; \ |v - r| > \omega \end{cases} \tag{13}$$

Here, the cutting-edge parameter is specified as ω, v indicates response variable, r implies predicted value and loss function's derivate is embodied as $v-r$.

$$B_N = \begin{cases} (1-\psi)\,|\,v-r\,| & ; v-r \le 0 \\ \psi\,|\,v-r\,| & ; v-r > 0 \end{cases} \tag{14}$$

where the distribution parameter is exemplified as ψ.

Additionally, GBM iteratively enhances the prediction of z from d regarding B by applying base learners, and hence the additive ensemble approach with size I is formed.

$$D_0(d) = \tau,\ D_\kappa(d) = D_{\kappa-1}(d) + \rho_\kappa \zeta_\kappa(d), \kappa = 1,...,I \tag{15}$$

Here, ζ_κ indicates the κ^{th} base model, iteration index is exemplified as κ, weight or coefficient of κ^{th} base model is represented as ρ_κ, τ signifies initial prediction, and here the final predicted outcome is indicated as P_i. Fig. 2 illustrates the GBM architecture.

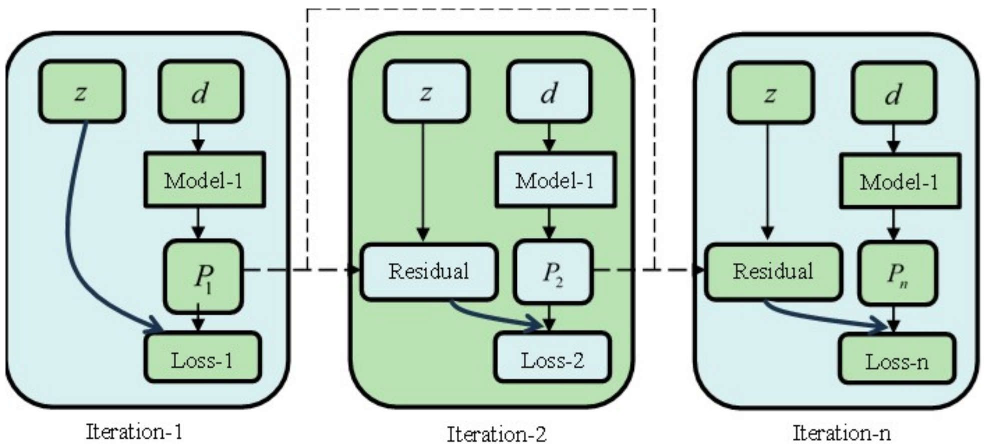

Fig. 2. *GBM architecture*

4. Result and Discussion

The investigational outcomes of GBM+HQLoss employed for weather forecasting with various measures are demonstrated in this section.

4.1 Dataset Description

Weather Dataset [16] comprises 12 columns, which include formatted data, summary, temperature, apparent temperature, humidity, wind speed, wind bearing, visibility, cloud cover, pressure, daily summary, and precip type. Here, the summary is based on two climates, such as partly cloudy and mostly cloudy.

4.2 Image Analysis

Fig. 3 illustrates the image results of GBM+HQLoss for various climatic conditions. Fig. 3(a) shows the image sample with a breezy climate. On 2008-01-28, the temperature is 3.311C and the apparent temperature is -2.127C. It can be visualized from the figure that the apparent temperature in a breezy climate was much lower than in the actual climate. In Fig. 3(b), the image sample of GBM+HQLoss based on Foggy climate is signified. Here, on 2008-11-15, the temperature and apparent temperature obtained are -1.711C and -4.038C. When the climate was foggy, the temperatures remained the same for most of the days. The image sample of GBM+HQLoss for a mostly cloudy climate is represented in Fig. 3(c). On 2008-06-19, the temperature and apparent temperature measured are 27.033C and 26.944C. As visualized from the figure, the apparent temperature was higher than the actual temperature on most days.

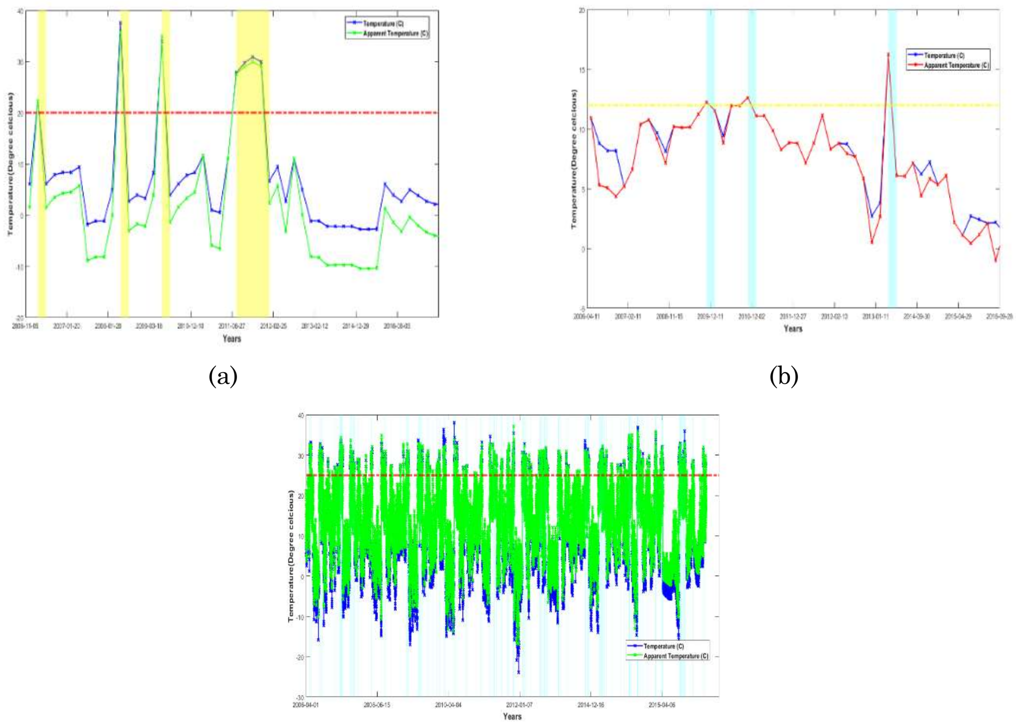

(a) (b)

(c)

Fig. 3. *Image results of GBM+HQLoss for (a) Breezy, (b) Foggy, and (c) Mostly cloudy*

4.3 Evaluation Metrics

The performance measures, like MAPE, RMSE, and MSE are utilized for examining the efficacy of GBM+HQLoss, and they are explained beneath.

a) MSE: To determine the average square difference between the original and assessed value, MSE is used. Here, the expression of MSE is designated as,

$$U = \frac{1}{m}\sum_{\upsilon=1}^{m}\left(P_i^* - P_i\right)^2 \tag{16}$$

Here, the original and assessed value obtained using GBM is denoted as P_i and P_i^*, MSE is implied as U, and the amount of training sample is designated as m.

b) RMSE: The square root of MSE is considered for calculating RMSE, which is represented as,

$$L = \sqrt{U} \tag{17}$$

where RMSE is exemplified as L.

b) MAPE: MAPE is utilized for assessing the accuracy of forecasting techniques, and it is referred to as the average absolute percentage difference between the original and assessed value. Moreover, MAPE is expressed as,

$$X = \frac{1}{m}\sum_{\upsilon=1}^{m}\left|\frac{P_i - P_i^*}{P_i}\right| \tag{18}$$

wherein, X represents the MAPE.

4.4. Performance Analysis

In Fig. 4, the examination of GBM+HQLoss based on various evaluation measures is shown. The graph plotted among delay and RMSE is displayed in Fig. 4(a). When the delay is 2000, the RMSE recorded by GBM+HQLoss for learning rates of 0.1, 0.01, 0.05, and 0.001 is 0.407, 0.383, 0.354, and 0.331. Fig. 4(b) depicts the investigation of GBM+HQLoss with MAPE. For a delay of 4000, the value of MAPE obtained by GBM+HQLoss with a learning rate of 0.1 is 0.288, 0.01 is 0.266, 0.05 is 0.258, and 0.001 is 0.248. In Fig. 4(c), the valuation of GBM+HQLoss to MSE is represented. At a delay of 3000, the MSE figured by GBM+HQLoss with learning rates of 0.1, 0.01, 0.05, and 0.001 is 0.138 0.117, 0.099, and 0.066.

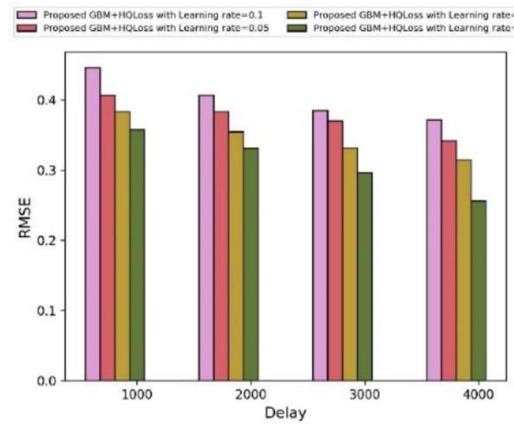

(a)

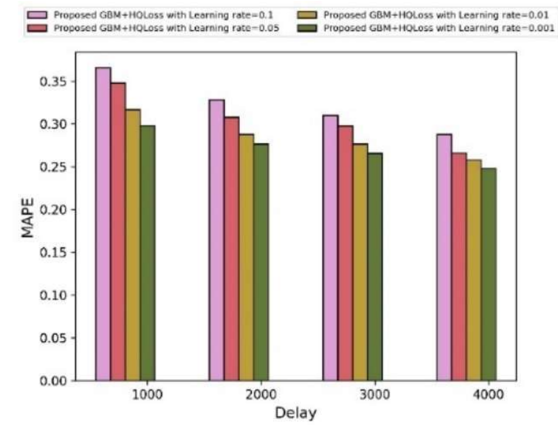

(b)

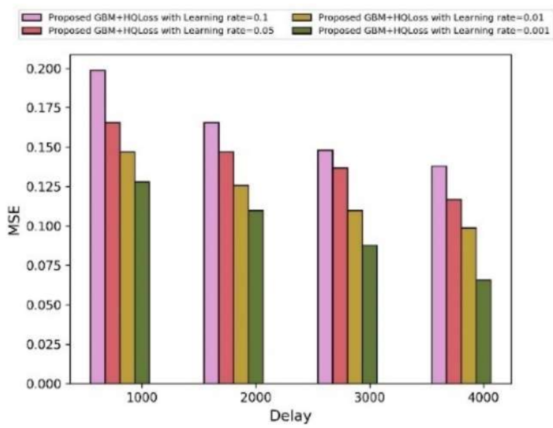

(c)

Fig. 4. *Performance examination of GBM+HQLoss with (a) RMSE, (b) MAPE, and (c) MSE*

4.5 Comparative Methods

Different prevailing techniques of weather forecasting are correlated with the newly introduced GBM+HQLoss technique for analyzing its efficacy. Here, the existing models, like Catboost+ST+FS+WPD [1], W-MAE [2], HiSTGNN [3], and SFA-LSTM [4] are considered.

4.6 Comparative Analysis

The graph drawn between delay and different performance measures is represented in Fig. 5. The evaluation based on RMSE is delineated in Fig. 5(a). Here, when considering the delay as 3000, the RMSE quantified by GBM+HQLoss is 0.296, while the prevailing models including Catboost+ST+FS+WPD, W-MAE, HiSTGNN, and SFA-LSTM recorded an RMSE of 0.487, 0.458, 0.407, and 0.343. In Fig. 5(b), the graph between MAPE and delay is portrayed. The MAPE calculated by GBM+HQLoss for delay 1000 is 0.298, where the MAPE obtained by Catboost+ST+FS+WPD is 0.418, W-MAE is 0.399, HiSTGNN is 0.367, and SFA-LSTM is 0.348. Fig. 5(c) signifies the investigation of GBM+HQLoss with MSE by changing the value of delay. For a delay of 4000, the MSE value measured by Catboost+ST+FS+WPD, W-MAE, HiSTGNN, SFA-LSTM, and GBM+HQLoss is 0.210, 0.188, 0.148, 0.098, and 0.066.

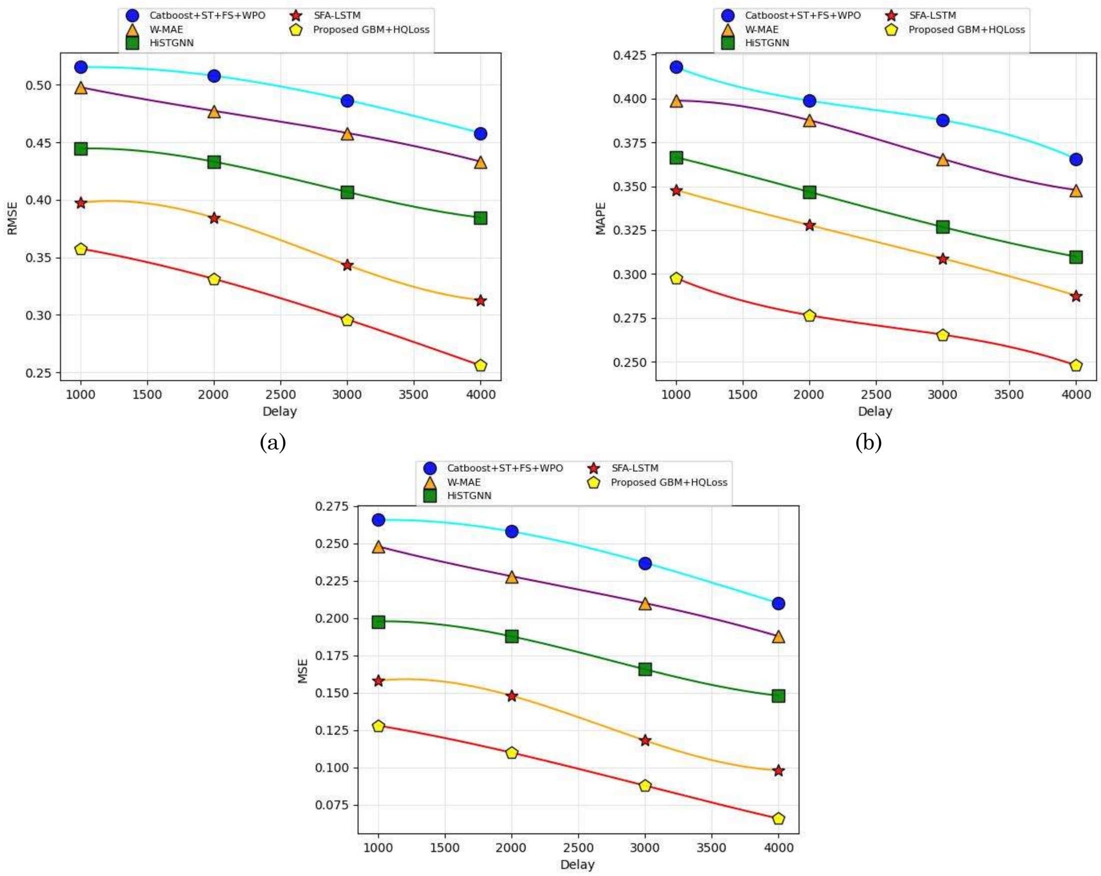

(c)

Fig. 5. *Comparative valuation of GBM+HQLoss with (a) RMSE, (b) MAPE, and (c) MSE*

4.7 Comparative Discussion

The comparative discussion of GBM+HQLoss for weather forecasting with various measures is shown in Table 1. Here, the newly presented GBM+HQLoss method computed a minimum RMSE of 0.256, MAPE of 0.248, and MSE of 0.066. Besides, the traditional models, like Catboost+ST+FS+WPD, W-MAE, HiSTGNN, and SFA-LSTM recorded a RMSE of 0.458, 0.433, 0.385, and 0.313, while these models calculated a MAPE of 0.366, 0.348, 0.310, and 0.288. Further, the MSE value attained by Catboost+ST+FS+WPD is 0.210, W-MAE is 0.188, HiSTGNN is 0.148, and SFA-LSTM is 0.098. Hence, it is observed that the GBM+HQLoss model obtained better performance than other approaches. Moreover, GBM is more flexible and robust to overfitting risks, and the HQ Loss function used for the tuning process of GBM enhanced the interpretability.

Table 1. *Comparative Discussion of GBM+HQLoss*

Metrics	Catboost+ST+FS+WPD	W-MAE	HiSTGNN	SFA-LSTM	Proposed GBM+HQLoss
RMSE	0.458	0.433	0.385	0.313	**0.256**
MAPE	0.366	0.348	0.310	0.288	**0.248**
MSE	0.210	0.188	0.148	0.098	**0.066**

5. Conclusion

Weather forecasting is a well-established computational challenge with economic impacts and the weather conditions are connected to all the fields of life and production. Moreover, due to the complexity of atmospheric movement and the uncertainty of weather conditions, the prediction of weather is challenging. Further, the conventional methods employed to predict weather leads to a high error rate because of the sudden climate change. Hence a new technique based on GBM+HQLoss is proposed for predicting the weather. Initially, the input time series data is passed to the extraction phase, where various technical indicators are mined from the data. Following this, the most significant features are selected based on IG, and lastly, the weather forecasting is executed by employing GBM+HQLoss. Here, the training process of GBM is performed using HQ loss, which is formulated by the integration of Huber loss and Quantile loss.

Furthermore, the GBM+HQLoss technique attained a minimum RMSE of 0.256, MSE of 0.066, and MAPE of 0.248. Future work aims to execute optimization models and DL for analyzing large databases to improve the prediction methods and identify complex weather patterns.

Compliance With Ethical Standards

Conflicts of interest: Authors declared that they have no conflict of interest.

Human participants: The conducted research follows ethical standards and the authors ensured that they have not conducted any studies with human participants or animals.

References

[1] D. Niu, L. Diao, Z. Zang, H. Che, T. Zhang, and Chen, X., "A machine-learning approach combining wavelet packet denoising with catboost for weather forecasting", Atmosphere, Vol.12, No.12, pp.1618, 2021.
[2] X. Man, C. Zhang, J. Feng, C. Li, and J. Shao, "W-mae: Pre-trained weather model with masked autoencoder for multi-variable weather forecasting", arXiv preprint arXiv:2304.08754, 2023.
[3] M. Ma, P. Xie, F. Teng, B. Wang, S. Ji, J. Zhang, and T. Li, "Histgnn: Hierarchical spatio-temporal graph neural network for weather forecasting", Information Sciences, vol.648, pp.119580, 2023.
[4] M.A.R. Suleman, and S. Shridevi, "Short-term weather forecasting using spatial feature attention-based LSTM model", IEEE Access, vol.10, pp.82456-82468, 2022.
[5] P. Hewage, M. Trovati, E. Pereira, and A. Behera, "Deep learning-based effective fine-grained weather forecasting model", Pattern Analysis and Applications, vol.24, no.1, pp.343-366, 2021.
[6] D. Kapgate, "Weighted moving average forecast model-based prediction service broker algorithm for cloud computing", International Journal of Computer Science and Mobile Computing, vol.3, no.2, pp.71-79, 2014.
[7] S. Gumparthi, "Relative strength index for developing effective trading strategies in constructing optimal portfolio", International Journal of Applied Engineering Research, vol.12, no.19, pp.8926-8936, 2017.
[8] S.M. Nor, and G. Wickremasinghe, "The profitability of MACD and RSI trading rules in the Australian stock market", Investment Management and Financial Innovations, vol.11, no.4, pp.194-199, 2014.
[9] S. Vergura, "Bollinger bands based on exponential moving average for statistical monitoring of multi-array photovoltaic systems", Energies, vol.13, no.15, pp.3992, 2020.
[10] T. Panapongpakorn, and D. Banjerdpongchai, "Short-term load forecast for energy management systems using time series analysis and neural network method with average true range", In Proceedings of 2019 First International Symposium on Instrumentation, control, artificial intelligence, and Robotics (ICA-SYMP), IEEE, pp. 86-89, January 2019.
[11] B. Prasetiyo, M.A. Muslim, and N. Baroroh, "Evaluation of feature selection using information gain and gain ratio on bank marketing classification using naïve bayes", In Proceedings of Journal of physics: conference series, IOP Publishing, Vol. 1918, No. 4, pp. 042153, June 2021,
[12] A.V. Konstantinov, and L.V. Utkin, "Interpretable machine learning with an ensemble of gradient boosting machines", Knowledge-Based Systems, vol.222, pp.106993, 2021.
[13] A. Natekin, and A. Knoll, "Gradient boosting machines, a tutorial", Frontiers in neurorobotics, vol.7, pp.21, 2013.
[14] J. Feng, Y.X. Xu, Y. Jiang, and Z.H. Zhou, "Soft gradient boosting machine", arXiv preprint arXiv:2006.04059, 2020.
[15] H. Shaiba, R. Marzouk, M.K. Nour, N. Negm, A.M. Hilal, A. Mohamed, A. Motwakel, I. Yaseen, A.S. Zamani, and M. Rizwanullah, "Weather Forecasting Prediction Using Ensemble Machine Learning for Big Data Applications", Computers, Materials & Continua, vol.73, no.2, 2022.
[16] The weather dataset is taken from https://www.kaggle.com/datasets/muthuj7/weather-dataset" accessed on October 2024.